Journal of Applied Polymer Science

Physico-Chemical, Thermal, and Mechanical Approaches for the Characterization of Solubilized and Solid State Chitosans

Narimane Mati-Baouche,[1] Hélène De Baynast,[1] Christophe Vial,[1] Fabrice Audonnet,[1] Shengnan Sun,[1] Emmanuel Petit,[2] Fabienne Pennec,[3] Vanessa Prevot,[4] Philippe Michaud[1]

[1]Clermont Université, Université Blaise Pascal, Institut Pascal UMR CNRS 6602, 24 avenue des Landais, BP-206, 63174 Aubière Cedex, France

[2]Laboratoire BIOPI, IUT d'Amiens (GB), Avenue des Facultés, le Bailly 80025, Amiens Cedex, France

[3]Laboratoire Groupe d'Etude des Matériaux Hétérogènes (GEMH-ENSCI EA 3178) Centre Européen de la Céramique, 12 rue Atlantis 87068, Limoges Cedex, France

[4]Clermont Université, Université Blaise Pascal, CNRS, UMR 6296, Institut de Chimie de Clermont-Ferrand, 24 avenue des Landais, BP 80026, 63171 Aubière Cedex, France

Correspondence to: P. Michaud (E-mail: philippe.michaud@univ-bpclermont.fr)

ABSTRACT: This study was conducted on the both solid and solubilized chitosans to propose an approach for the physico-chemical, thermal and mechanical characterizations of this polysaccharide. The polysaccharide used was a 90% deacetylated chitosan having a molecular weight of 98.4 kDa. The flow property of chitosan solutions was evaluated revealing a shear-thinning behavior. The thermal characterization was carried out by studying heat specific capacity, glass transition temperature, and thermal conductivity on chitosan dried specimens (solid state). Their T_g were measured by DSC and confirmed by DMA at 102 and 122°C depending on concentrations of initial chitosan solutions. The mechanical characterization was conducted by analyzing Young modulus, tensile strength, and elongation at break of chitosan specimens. They exhibited a higher elongation at break and a lower tensile strength when made from high concentrated chitosan solution (9% w/v). Differences in mechanical behavior of specimens were explained by differences of crystallinity. © 2014 Wiley Periodicals, Inc. J. Appl. Polym. Sci. **2015**, *132*, 41257.

KEYWORDS: adhesives; biodegradable; biopolymers and renewable polymers; mechanical properties; polysaccharides

Received 8 February 2014; accepted 29 June 2014
DOI: 10.1002/app.41257

INTRODUCTION

Chitosan is a polysaccharide obtained by alkaline deacetylation of chitin. This heteropolymer of β-(1,4)-linked 2-acetamido-2-deoxy-D-glucopyranose and 2-amino-2-deoxy-D-glucopyranose is the sole natural cationic polysaccharide due to its positive charges (NH_3^+) at acidic pH (pH < 6.5).[1] During the past several decades, chitosan has received a great attention in the area of biomaterials and/or biobased materials.[2,3] A biobased material is a material made from biomass whereas "biomaterial" designed biocompatible material used in the medical field. The commercial availability of chitosans open the way to the development of these materials notably in the field of films and adhesives.[4,5] In this context, even if thermal, mechanical, and structural studies have been currently published for the characterization of chitosans, the literature is actually highly heterogeneous. Effectively no publication described the fully rheological, thermal, and mechanical characterizations of a structurally defined chitosan in both liquid and solid states (global approach). In the majority of cases authors studied only some of these aspects on a defined film or on a solution of chitosan. This lack of global physico-chemical study of a well-defined chitosan in liquid and solid states associated to the large variety of chitosan origins (lobster, crab, and fungi) with specific molecular characteristics (degree of deacetylation, molecular weight)[6] and applications explain the heterogeneity of literature about this subject. For example, considering mechanical properties of chitosan films, data varied widely ranging from 7 to 50 MPa for tensile strength, from 9.6 MPa to 2.1 GPa for Young modulus and from 5 to 65% for strain at break.[7–10] The thermal behavior of chitosan, evaluated by differential scanning calorimetry (DSC) measurements, was also abundantly described in literature. However, the results obtained were various and subject to controversy[11] as some authors could not evaluate T_g of chitosan,[12,13] whereas others observed it ranging from −23 to 222°C.[14–17] Moreover, thermal conductivity (κ) and specific heat (C_p) of chitosan dried specimens, such as films are not described at this time despite the importance of these

parameters in biobased materials and biomaterials applications. In addition, all literature found about the characterization of chitosan is established using low concentrated solutions and no data described the behavior of this polysaccharide for concentrations above 20 g L^{-1}. In this context, it is actually difficult to correlate all the physico-chemical properties of a defined chitosan both in liquid and solid states and to compare the obtained results with literature. Hence, the aim of this study is firstly to propose a defined and standardized procedure (global approach) to obtain a fully physico-chemical characterization of chitosans (both liquid and solid states) using adapted analytical methods. This procedure, applied to an unknown sample of chitosan, should allow to compare it with others chitosans fully characterized and to employ it or not in some biomaterial and/or biobased material fields in regard to its performances. Secondly, data collected in this study give new information and physico-chemical values which can complete basic aspects about this polysaccharide mostly when it's highly concentrated.

EXPERIMENTAL

Materials

Chitosan from shrimp shell with a deacetylation degree (DD) of 90% was supplied by France-Chitin (France) with the reference number 342. All other chemicals used in this study were analytical grade reagents (Sigma-Aldrich).

Sample Preparation

Chitosan solutions with concentrations between 0.1 and 1% (w/v) were made in 0.1% (v/v) acetic acid, whereas those with concentrations between 2 and 4% (w/v) were made in 1% (v/v) acetic acid. Finally, chitosan solutions with concentrations between 4 and 9% (w/v) were prepared using 2% (v/v) acetic acid as solvent.

To obtain dried chitosan specimens, chitosan solutions at 4% (w/v—specimen *A*) and 9% (w/v—specimen *B*) were centrifuged (12,000 rpm, 30 min, 10°C) and 200 mL of supernatants were applied in a specific polypropylene rectangular mold (size: 90 mm × 90 mm × 40 mm) before being dried at 40°C during 72 h.

Characterization of Solubilized Chitosan

Molecular Weight Determination. The average molecular weight of chitosan was determined by high pressure size exclusion chromatography (HPSEC) with online multiangle laser light scattering (MALLS) filled with a K5 cell (50 μL) and two detectors: an He–Ne laser ($\lambda = 690$ nm) and a differential refractive index (DRI) as described previously.[4] The columns [OHPAK SB-G guard column, OHPAK SB806, 804, and 803 HQ columns (Shodex)] were eluted with 65 μM ammonium acetate (pH 4.5) at 0.7 mL min^{-1}. The solvent was filtered through 0.1 μm filter, degassed, and finally filtered through a 0.45 μm filter upstream column. The specimen was injected through a 100 μL full loop. The collected data were analyzed using the Astra 4.50 software package.

Viscosity and Critical Overlap Concentration Determinations. The critical overlap concentration (C^*) represents the limit between dilute and semidilute regimes. Over C^*, i.e., in the semidilute regime, polysaccharide entanglements are more important and polymers are more sensitive to physical stress. C^* was deduced using rheology. Apparent viscosity measurements were carried out using double concentric cylinder geometry with a stress-controlled rheometer AR-G2 (TA Instruments, France) equipped with a Peltier temperature control system. Temperature was set at 20°C and viscosity was monitored in the range of shear rate ($\dot{\gamma}$) : 10^{-2}–10^{2} s^{-1}. Each solution of chitosan was measured twice. Dynamic viscoelastic measurements were also performed using the same rheometer on liquid state chitosans, using parallel plate shear mode to measure the storage modulus (or elastic modulus), G' (Pa) and the loss modulus (or viscous modulus), G'' (Pa). The linear viscoelastic region was determined using strain sweep tests. Mechanical spectra between 0.01 and 10 Hz at 5% strain were recorded at 20°C, and temperature ramp tests were carried out between 10 and 40°C at 5% strain and 5 Hz to analyze the effect of temperature. 3 mL of dexadecane were poured into the samples before each analysis to avoid water and acetic acid evaporations. Viscosity data were collected and analyzed using the *Rheology Advance* software package and the Williamson model (1).[18]

$$\eta = \frac{\eta_0}{(1+(k\dot{\gamma})^n)} \quad (1)$$

where η is the apparent viscosity, η_0 the Newtonian solvent viscosity, k the time constant (s), and n the flow index.

C^* was deduced from the log–log plot of the specific viscosity vs. polymer concentration. The break in the slope gave access to C^*. Specific viscosity η_{sp} was calculated by the following eq. (2):

$$\eta_{sp} = \frac{(\eta_0 - \eta_s)}{\eta_s} \quad (2)$$

where η_s is the solvent viscosity (in this case, water $\eta_s = 0.001$ Pa s).

Characterization of Chitosan Solid State

Water Content Determination. Infrared balance (Precisa HA300) was used to evaluate water content of chitosan dried specimens (1 g crushed samples using a mortar) measuring the loss of weight in a range of temperature from 25 to 150°C at a heating rate of 2°C min^{-1}.

Thermogravimetric analyses (TGA) were recorded on solid state specimens *A* and *B* (5–20 mg) in an inert atmosphere with a Setaram TG-DTA 92 instrument in the temperature range of 25–1000°C, with a heating rate of 5°C min^{-1}.

Thermal Properties Determination. The thermal properties of the specimens *A* and *B* were characterized by a differential scanning calorimeter (DSC 2920, TA Instruments, France) under nitrogen atmosphere. DSC instrument was calibrated with indium standard. Glass temperature transition T_g (°C) represents the transition between solid and viscous phases for chitosan dried specimens and was measured using two runs. Samples were firstly heated from 0 to 150°C at a heating rate of 10°C min^{-1} to evaporate water. After that they were cooled at 0°C at a cooling rate of 10°C min^{-1} and were reheated until reaching 250°C for the second run with a heating rate of 10°C min^{-1}. The T_g was taken as the midpoint of heat capacity change during heating second run. With the aim to determine

chitosan's heat capacity C_p (J g^{-1} K^{-1}), samples in hermetic aluminium pans were heated from 0 until 50°C with a heating rate of 1°C min^{-1}. The C_p values at 20°C were taken by the following eq. (3):

$$C_{p(20°C)}(\mathrm{J\,g^{-1}K^{-1}}) = \frac{\varphi_{20°C}(\mathrm{mW}) \times 60(\mathrm{s\,K^{-1}})}{m(\mathrm{mg})} \quad (3)$$

where φ represents heat flow and m represents the weight of the sample (around 10 mg).

Flash laser method permits to evaluate the thermal diffusivity α (mm^2 s^{-1}) of dried specimens. Assuming that the samples behave as a homogeneous medium, knowing ρ (kg m^{-3}), the measured apparent density of dried chitosan specimens, and measuring α and C_p, the thermal conductivity (κ) is obtained by the expression (4):

$$k = \alpha \rho C_p \quad (4)$$

Mechanical Properties Determination. Rectangular specimens (30 mm × 5 mm × 0.9 mm) of dried specimens *A* and *B* were tested on tensile mode. A microtensile machine (Deben^{TM}) with a crosshead speed of 5 mm min^{-1} was used firstly to obtain stress–strain curves of strip shaped dried specimens. Stress–strain curves present typically two areas. One corresponds to the deformation (elongation) which is proportional to the stress and corresponds to an elastic reversible train. The other one represents the area when the strain is nonlinear and irreversible corresponding to a plastic area. The tensile strength (TS) (MPa) and the strain at break ε_b (%) (percentage of elongation at break) were measured in a static mode. The measurements were replicated three times. A second method used was the Dynamic Mechanical Analyser (DMA 2980, TA Instruments, France). In a dynamic mechanical test, sample undergoes a longitudinal deformation due to a sinusoidal stress causing a complex modulus (E^*) expressed by eq. (5):

$$E^* = E' + iE'' \quad (5)$$

where E' (GPa) is the real component which represents the elastic modulus (Young modulus or storage). i is the imaginary unit ($i^2 = -1$), and E'' the imaginary component representing the loss modulus. E' and E'' were measured at a frequency of 1 Hz over the temperature ranging from 25 to 250°C with a heating rate of 10°C min^{-1}. The phase shift between stress and deformation of the sample is expressed with an angle δ. The loss factor of the sample is expressed by tangent of the angle δ "tan δ" (6) and corresponds to the resulting damping of the material.

$$\tan\delta = \frac{E''}{E'} \quad (6)$$

Physico-Chemical Properties Determination. Crystallinity of specimens *A* and *B* (32 mm of diameter) was determined by X-ray diffraction and infrared spectrometry measurements.

X-ray diffraction analyses were recorded on an X'Pert Pro Philips diffractometer with diffracted beam graphite monochromator using Cu-Kα radiation source in the 2θ range of 2°–50° with a step of 0.017° and a counting time per step of 500 s. Crystallinity index (% *I*) was determined by the method of Focher et al.[19] using eq. (7).

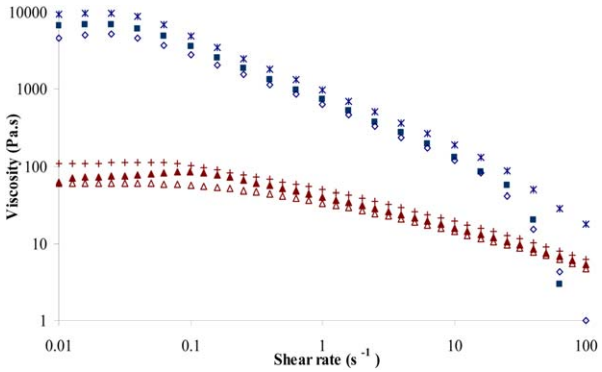

Figure 1. Influence of the shear rate and temperature on the rheological properties of chitosan solution. +, ▲, △: chitosan 4% (w/v) at 15, 20, and at 30°C, respectively. x, ■, ◇: chitosan 9% (w/v) at 15, 20, and at 30°C, respectively. Maximum standard deviation for solutions of chitosan 4% at 15, 20, and 30°C : ±12. Maximum standard deviation for solutions of chitosan 9% at 15, 20, and 30°C : ±15. [Color figure can be viewed in the online issue, which is available at wileyonlinelibrary.com.]

$$\%I = \left(\frac{I_c - I_a}{I_c}\right) \times 100 \quad (7)$$

where maximum intensity to lattice diffraction, I_c, was measured at $2\theta = 20°$ for the lattice diffraction and the amorphous region diffraction, I_a, at $2\theta = 16°$.

Attenuated total reflectance Fourier transform infrared (FT-IR) spectra were measured in the range of 400–2000 cm^{-1} on a FTIR Nicolet 5700 Spectrometer (Thermo Electron Corporation) equipped with a Smart Orbit accessory. All readings were performed at room temperature (20°C).

RESULTS AND DISCUSSION

Physico-Chemical Characterization of Chitosan in Solution

The molecular weight of chitosan used in this study was estimated to 98.42 kDa with a polydispersity (M_w/M_n) of 1.135 ± 0.075 by SEC MALLS analysis. This result was in agreement with other commercial chitosans having M_w ranging between 100 and 1500 kDa.[20] Its rheological behavior was analyzed using variably concentrated solutions with shear rate swept from 0.01 to 100 s^{-1} (Figure 1). Solutions had shear-thinning behavior. Below a critical shear rate value, the flow curve shows an initial region: the low-shear Newtonian plateau where the viscosity keeps a constant value η_0. Then, a shear-thinning region emerges in which viscosity decreases when shear rate increases, following a power-law behavior. At high shear rate, viscosity tends to a second Newtonian plateau η_∞. This kind of behavior reflects the influence of shear on the entanglement density of chitosan chains. Above a threshold, shear tends to disentangle polymer chains and, as a consequence, viscosity decreases until a minimum value is achieved. Chitosan solutions present Newtonian plateau for each concentration of polysaccharide at low shear rates ($\dot{\gamma} < 0.01$ s^{-1}). Williamson model has been used to fit experimental results of apparent viscosity versus shear rate. The parameters of the model were for solutions of chitosan at 4 and 9% at 20°C: $\eta_0 = 90.2$ Pa s, $n = 1.3$, and $\eta_0 = 7132$ Pa s, $n = 1$, respectively. In a second step, the specific viscosity was measured with different polysaccharide

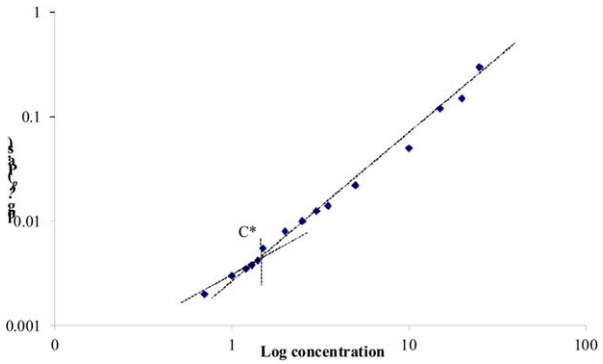

Figure 2. Critical concentration of chitosan (C^*) obtained after log–log plot of the specific viscosity η_{sp} (Pa s) versus polymer concentration (g L^{-1}). [Color figure can be viewed in the online issue, which is available at wileyonlinelibrary.com.]

concentrations to evaluate the C^* of this polysaccharide. C^* was 1.45 g L^{-1} (0.145 %) at 20°C (Figure 2). This value was similar to that evaluated by Argüelles–Monal et al.[21] with a chitosan having a *DD* of 80%. Knowing the C^* of chitosan the influence of both temperature and concentration about viscosity in semi-diluted regimes were studied (Figure 1). Logically, the viscosity increased with concentration and decreased with temperature as previously described by other authors.[22] This information is important in the field of films[23,24] and adhesives[25] where the chitosan is carried out at liquid state. In this context the control of viscosity and so application on adherents of chitosan solutions are necessary. In addition, the results of oscillatory shear tests show that 4 and 9% chitosan solutions exhibit a viscoelastic linear region up to 80 and 100% strain, respectively. Mechanical spectra at 20°C highlight that tangent loss, equal to G''/G', is about 2 for chitosan solutions at 4%, while it is close to 0.5 for chitosan solution at 9%. Both exhibit typical frequency-dependent viscoelastic behavior. Solutions of chitosan at 4% behaves as a viscoelastic liquid in Figure 3, while the parallel straight lines in the same figure for 9% chitosan solutions correspond to a physical gel. Silva-Weiss et al.[25] have mentioned that physical gels could have many applications as drug delivery agents and gelling hydrocolloids. They could also enhance the hardness, adhesiveness, and viscoelastic properties of the film forming solution. The increase of concentration favors the rise

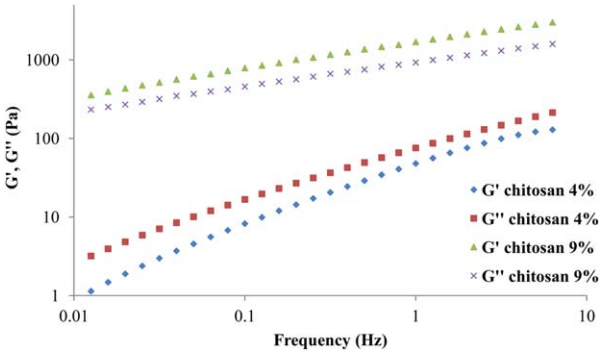

Figure 3. Log–log plot of elastic modulus (G') and loss modulus (G'') as a function of frequency for both chitosan 4 and 9%. [Color figure can be viewed in the online issue, which is available at wileyonlinelibrary.com.]

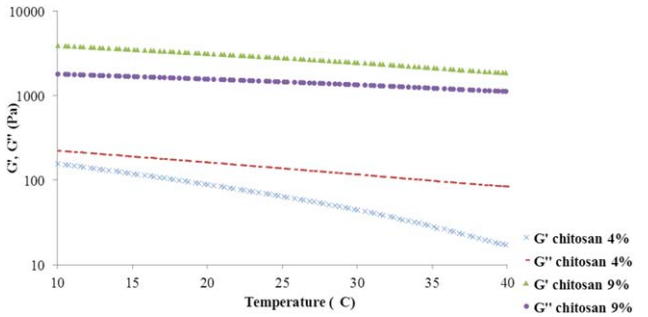

Figure 4. Elastic modulus (G') and loss modulus (G'') as a function of temperature for both chitosan 4 and 9%. [Color figure can be viewed in the online issue, which is available at wileyonlinelibrary.com.]

of the storage modulus G', which can be attributed to the presence of more polymer entangled chains,[26] whereas the increase of the viscous modulus remains four times smaller. Concerning the influence of temperature, Figure 4 shows that both storage and loss moduli decrease when temperature increase, as expected, which confirms the decrease of the zero-shear viscosity η_0 observed in Figure 1 as a function of temperature. G' decreased more rapidly than G'' for both polymer concentrations, which emphasizes a strong effect of temperature on polymer entanglement.

Physico-Chemical Characterization of Chitosan in Solid State

Chitosan is currently used for tissue engineering,[27] food packaging,[3] as adhesive,[4] and for film preparation.[14] So, the thermal and mechanical characterizations of solid state chitosan are necessary to predict its behavior in specific environments.

Determination of Water Content. The moisture content is related to the total void volume occupied by water molecules in the network microstructure of a chitosan film.[28] Moreover water content has a significant influence on physical properties of chitosan acting as plasticizer.[11] For all these reasons, the evaluation of water content of the dried specimens before their thermal degradation was performed. Water content was evaluated for specimens *A* and *B* at 13 and 13.5%, respectively with Infrared (IR) balance, and at 9.2 and 7.1%, respectively by TGA measurements when reaching 150°C (the same limit in temperature using IR balance) (Figure 5). These amounts are in agreement with the percentages found by Lopez et al.[29] and Rubilar et al.[30] The differences of results obtained by infrared balance and TGA measurements could be explained by the nature of chitosan samples (powder of specimens for infrared balance and sheet of specimen for TGA), but also by the heating rates which are not the same in the two methods.

Characterization of Thermal Properties. Since chitosan is exploited and used in the field of biomaterials, it is important to define its mechanical performances as a function of temperature. Its behavior depending on temperature is not well described in literature and controversies exist notably for the value of its glass transition. Moreover, its thermal conductivity (κ) which is an important parameter for different application fields, such as tissue engineering and insulating materials, has not been described at this time.

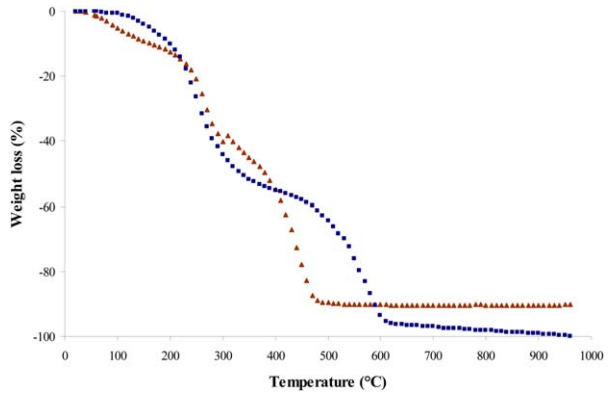

Figure 5. TGA curves of chitosan's specimens *A* (▲) and *B* (■). [Color figure can be viewed in the online issue, which is available at wileyonlinelibrary.com.]

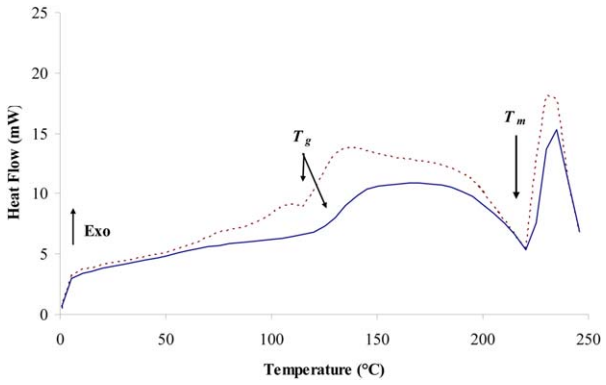

Figure 6. DSC second run curves of chitosan specimens *A* (·····) and *B* (——); T_g is the glass transition temperature, T_m is the melting temperature. [Color figure can be viewed in the online issue, which is available at wileyonlinelibrary.com.]

In a first time, chitosan dried specimens were characterized using DSC. Both specimens *A* and *B* exhibited a broad exothermic peak centred at 80°C in the first run of DSC (data not shown). This peak is attributed to the loss of water associated with the hydrophilic groups of the polymer.[31] The second run is shown in Figure 6. It gives access to glass transition temperature T_g and melting point (T_m) of both chitosan specimens. Table I summarizes all thermal properties of chitosan specimens obtained using DSC (C_p, T_g, T_m) and completed with TGA analysis (T_d) and flash laser (α, κ).

T_g of chitosan specimens obtained from solution of 4% (w/v) and 9% (w/v) were respectively 102°C and 135°C (Figure 6). These values are in agreement with those reported by Cheung et al.[31] (103°C) for the specimen *A* but not for the specimen *B*. However, Dong et al.[16] estimated T_g of chitosan film at 140–150°C. Regarding the literature, some authors could not evaluate T_g of chitosan[12,13] while others observed it ranging from −23 to 67°C,[14] at 30°C,[32] near to 100°C,[33] between 130 and 150°C[15,16] and between 194 and 196°C.[34] Other authors described it up to 208°C.[17,35] The main reason for these heterogeneous results may be attributed to some specific features of tested chitosans, such as their origin, molecular weight, deacetylated degree, and crystallinity.[6] The processes used to prepare films affects also thermal behavior of chitosan. In addition, wide variations can occur in chitosan films from solutions with different concentrations as observed in this study.

A peak was observed at 225°C (Figure 6) for both specimens corresponding to the thermal degradation of the polymer with vaporization of volatile compounds. This result was confirmed by TGA curves where a lost in weight is observed at the same temperature (Figure 5). Lopez et al.[29] explained that chitosan degradation occurs in three steps between 42–125, 268–312 and 387–471°C. The first step is not really a degradation, but rather a loss of water. The degradation between 268 and 312°C (second step) is associated with the breaking down of the polymeric chain. Finally the third effect (387–471°C) corresponds to the residual crosslinked degradation of chitosan. The total degradation was evaluated by TGA at respectively 500 and 600°C for specimens *A* and *B*. These values correspond to those measured by Martinez-Camacho et al.[36]

Thermal conductivity of chitosan (κ) was determined by flash laser method. Results found are 0.21 and 0.40 W m^{-1} K^{-1} for chitosan specimens *A* and *B*, respectively. It is necessary to quantify this parameter for materials with insulating properties. A polymer with κ below 0.1 W m^{-1} K^{-1} is considering insulator which is not the case for the chitosan used in this study. Note that no data are available in literature for the determination of these parameters on chitosan films.

Mechanical and Structural Properties of Chitosan Specimens. Mechanical properties are of primary importance to quantify the performances of materials expected to undergo various types of stresses during use. So the chitosan specimens were evaluated using both static and dynamic approaches. Figure 7 shows the stress–strain curves of chitosan specimens. The Table I summarizes the results obtained from micro-tensile machine and notably TS (in MPa) indicating the maximum tensile stress that the specimen can sustain, elongation at break (ε_b in %) which is the maximum change in the length of a test specimen

Table I. Apparent Density, ρ, Heat Specific C_p at 20°C, Glass Transition Temperature, T_g, Degradation Temperature, T_d, Thermal Diffusivity, α, Thermal Conductivity, λ, Strain at Break or Elongation, ε_b, Tensile Strength, TS, and Young Modulus, E' of Chitosan Specimens as a Function of Polymer Concentration During Film Forming

Chitosan's specimen	Thermal properties						Mechanical properties		
	ρ (kg m^{-3})	C_p (J g^{-1} K^{-1})	T_g (°C)	T_d (°C)	α (mm^2 s^{-1})	κ (W m^{-1} K^{-1})	ε_b (%)	TS (MPa)	E' (GPa)
A	796	1.61	102	500	0.14	0.21	5	71	4
B	1230	2.01	135	600	0.16	0.40	11	45	2.5

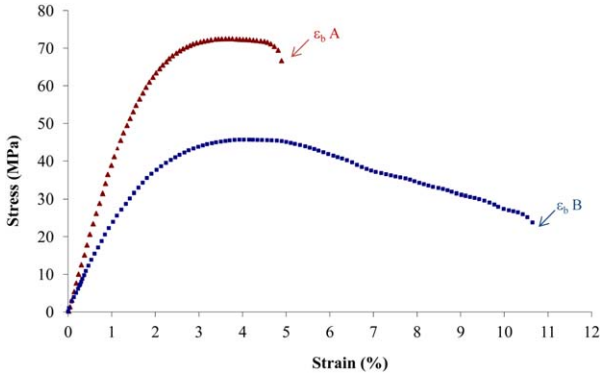

Figure 7. Typical stress–strain curves recorded from chitosan specimens *A* (▲) and *B* (■). [Color figure can be viewed in the online issue, which is available at wileyonlinelibrary.com.]

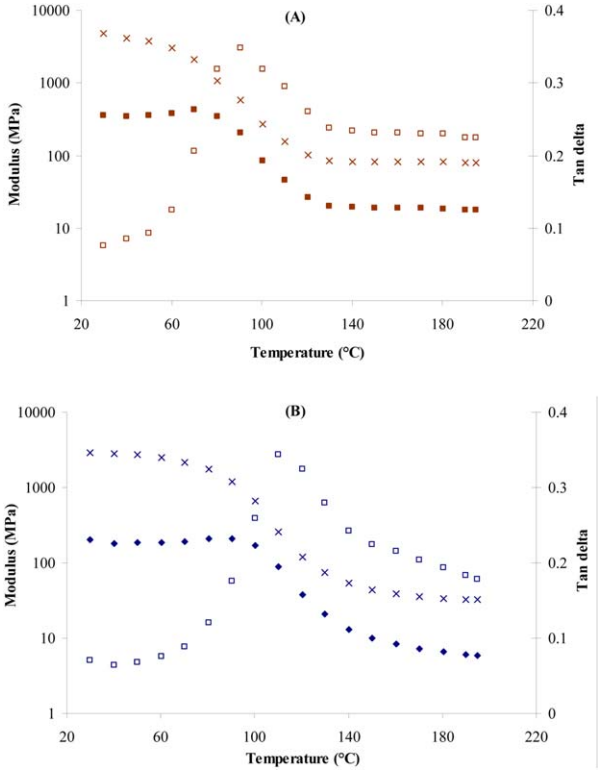

Figure 8. Mechanical analysis (DMA) in tensile dynamic mode obtained on chitosan specimen *A* (A) and chitosan specimen *B* (B) at 1 Hz frequency, (*x*) represents storage modulus, (■) represents loss modulus and (□) represents tangent δ. [Color figure can be viewed in the online issue, which is available at wileyonlinelibrary.com.]

before being broken and the elastic modulus (or Young modulus E' in GPa) corresponding to the stiffness of the specimen. It was observed that E' decreased in specimen *B* compared to specimen *A* from 4 to 2.5 GPa and regarding the TS, it decreased from 71 (specimen *A*) to 45 MPa (specimen *B*) reflecting a rigid behavior higher for the specimen *A*. Moreover, ε_b increased from 5 to 11% reflecting a larger plastic domain for the specimen *B* but also a brittle behavior. Uragami et al.[37] explain that during the film formation, hydrogen, bonding in the chitosan films increased with the increasing amount of amino and hydroxyl groups due to the increase in concentration of chitosan. The increasing of hydrogen bonds between hydroxyl groups and amino groups in the specimen *B*, compared to specimen *A* could explain the plastic behavior of the specimen *B*. Using DMA results, Young modulus was also evaluated at 4 GPa at 25°C for specimen *A* and at 2.7 GPa for specimen *B*. These results confirmed the previous ones obtained on microtensile machine, but are significantly different from those in the literature. Even if specimens *A* and *B* have larger thickness (0.9 mm) as compared to those of films described in literature (always inferior to 0.1 mm), the results are given in MPa to be independent from the dimensions of samples. Khoshgozaran-Abras et al.[7] measured on raw chitosan film a tensile strength (TS), an elongation at break (ε_b) and an elastic modulus (E') of 7.89 MPa, 65% and 9.62 MPa, respectively. Park et al.[10] found a TS and an ε_b of respectively, 40 MPa and 11% similar to the specimen *B*, whereas Leceta et al.[8] described a TS of 61 MPa and an ε_b of 5.6% which is similar to results obtained for the specimen *A*. Moreover, for Ma et al.[9] the TS and E' of raw chitosan film were measured at 64 MPa and 2.1 GPa, respectively. In the same way, Chen et al.[38] found a TS at 43.3 MPa. So the specimen *A* obtained from a solution of chitosan at 4% (w/v) presents better mechanical results (in term of rigidity) than the other films regarding both *TS* and E'.

On the other hand, Figure 8 shows the temperature dependence of the storage modulus (E') and loss modulus (E'') and damping tan δ of specimens *A* and *B* at a frequency of 1 Hz obtained from the DMA. A large peak can be seen in the tan δ near 100°C for specimen *A* and another is seen around 122°C for specimen *B*. These temperatures are in agreement with the glass transition temperature (T_g) estimated by DSC and mentioned above. They can be attributed to the α-relaxation of chitosan.[39] Mucha and Pawlak[33] reported that the α-relaxation of chitosan in the region of glass transition temperature depends on water acting as a plasticizer. A broad water evaporation peak in the vicinity of 100–130°C covers T_g of water-plasticized chitosan. Neto et al.[11] explained this phenomenon by the residual water present in all 'dried' samples acting as plasticizer and decreasing chitosan's T_g. However, Sakurai et al.[17] observed a peak at 153°C from DMA first run in pure chitosan. They associated that value to a local molecular motion in the pseudo-stable state. They also associated DMA measurements in a second heating run to α-relaxation at the same temperature as the T_g observed in DSC at 203°C.

Structural characterization was achieved to complete this study and to understand the difference observed between mechanical properties of specimens *A* and *B*. In the solid state, chitosan is a semicrystalline polymer.[40] Several crystalline polymorphic forms of chitosan have been reported in the literature. All having an extended twofold helical structure, but differing in packing density and water content. Figure 9 represents X-ray diffractograms of specimens *A* and *B*. The peaks of the chitosan specimens at around $2\theta = 12°$ and 20° were attributed to the diffraction from the chitosan acetate crystal planes of (100) and (020), respectively[13] in an orthorhombic system.[20] According to the

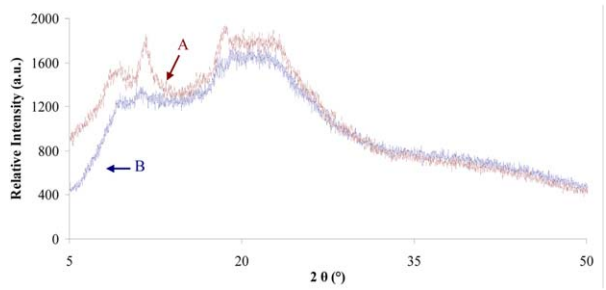

Figure 9. X-ray diffractogram of chitosan's specimens *A* and *B*. [Color figure can be viewed in the online issue, which is available at wileyonlinelibrary.com.]

literature, the reflection at $2\theta = 12°$ (near 10°) was assigned to crystal form I and the stronger reflection appeared at $2\theta = 20°$ corresponded to crystal form II.[9] On the first halo ($2\theta = 12°$), the crystallinity index (% *I*) determined by the method of Focher et al.[19] was calculated at 18% for the specimen *A* and 5% for the specimen *B*. This difference in crystallinity index observed at around 10° (peak I) was attributed to the hydrated crystalline structure of chitosan[41] because it is known that dried chitosan always contains bound water (5%).[30] X-ray results reflect that the specimen *B* was more amorphous than the specimen *A* and explain, accordingly, the highest rigidity of the specimen *A*. On the second halo ($2\theta = 20°$), no difference in crystallinity was observed and the both specimens presented a *% I* of 25%. This value was reported to be an indication of the relatively regular crystal lattice in chitosan.[41]

Figure 10 shows the FTIR spectra of specimens *A* and *B*. The main adsorption peaks of both specimens were observed at 1650 cm^{-1} [C═O stretching (amide I)], 1558 cm^{-1} [N─H bending (amide II)], and 1382 cm^{-1} [C─N stretching (amide III)].[8] Positions and absorption intensities of the bands were comparable and typical of chitosan.[42]

CONCLUSIONS

This study investigated the physico-chemical characterization of chitosan with the aim to complete information available about this polysaccharide and to develop an approach of characterization in liquid and solid states. Results show that chitosan solutions exhibit a shear-thinning behavior explained by the disorientation and disentanglement of the macromolecular chains under influence of shear rate. T_g of chitosan specimens were measured by DSC and confirmed by DMA at 102 and 122°C depending on concentrations of chitosan solution used and depending on water content. Differences in mechanical behavior of specimens obtained from variably concentrated solutions of the same chitosan were also observed in term of TS, ε_b, and E'. These differences were explained by differences of crystallinity.

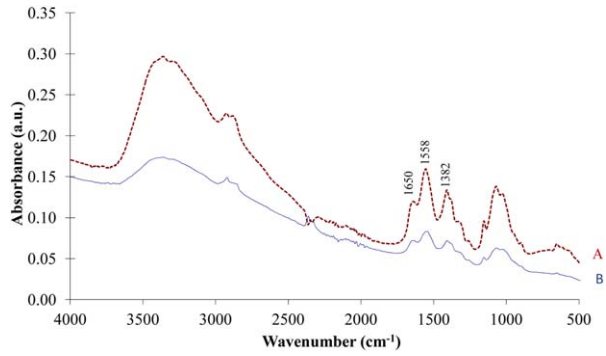

Figure 10. FT-IR spectra of chitosan specimens *A* (·····) and *B* (——). [Color figure can be viewed in the online issue, which is available at wileyonlinelibrary.com.]

ACKNOWLEDGMENTS

This work was supported by the French National Research Agency (ANR-DEMETHER-10-ECOT-004 grant), Céréales Vallée and Viaméca.

REFERENCES

1. Barbosa, M. A.; Granja, P. L.; Barrias, C. C.; Amaral, I. F. *ITBM-RBM* **2005**, *26*, 212.
2. Dash, M.; Chiellini, F.; Ottenbrite, R. M.; Chiellini, E. *Prog. Polym. Sci.* **2011**, *36*, 981.
3. No, H. K.; Meyers, S. P.; Prinyawiwatkul, W.; Xu, Z. *J. Food Sci.* **2007**, *72*, 87.
4. Patel, A. K.; Michaud, P.; Petit, E.; De Baynast, H.; Grédiac, M.; Mathias, J. D. *J. Appl. Polym. Sci.* **2013**, *127*, 5014.
5. Shalaby, W. S.; Dubose, J. A.; Shalaby, M. In Absorbable and Biodegradable Polymers; Shalaby, W. S.; Burg, K. J. L., Eds.; CRC Press: Boca Raton, **2004**; Chapter 7, p77.
6. Balau, L.; Gabriela, L.; Popa, M. I.; Tura, V.; Melnig, V. *Cent. Eur. J. Chem.* **2004**, *2*, 638.
7. Khoshgozaran-Abras, S.; Hossein Azizia, M.; Hamidya, Z.; Bagheripoor-Fallahb, N. *Carbohydr. Polym.* **2012**, *87*, 2058.
8. Leceta, I.; Guerrero, P.; de la Caba, K. *Carbohydr. Polym.* **2013**, *93*, 339.
9. Ma, B.; Li, X.; Qin, A.; He, C. *Carbohydr. Polym.* **2013**, *91*, 477.
10. Park, S. Y.; Park, H. J.; Lin, X. Q.; Sano, Y. *Hydrocolloid. Part I* **2000**, *199*.
11. Neto, C. G. T.; Giacometti, J. A.; Job, A. E.; Ferreira, F. C.; Fonseca, J. L. C.; Pereira, M. R. *Carbohydr. Polym.* **2005**, *62*, 97.
12. Sun, G.; Zhang, X.-Z.; Chu, C.-C. *J. Mater. Sci. Mater. Med.* **2007**, *18*, 1563.
13. Zhao, J.; Han, W.; Chen, H.; Tu, M.; Zeng, R.; Shi, Y.; Cha, Z.; Zhou, C. *Carbohydr. Polym.* **2011**, *83*, 1541.
14. Lazaridou, A.; Biliaderis, C. G. *Carbohydr. Polym.* **2005**, *48*, 179.
15. Cervera, M. F.; Heinamaki, J.; Rasasen, M.; Maunu, S. L.; Karjalaienen, M.; Nieto Acosta, O. M.; Iraizoz Colarte, A.; Yliruusi, J. *Carbohydr. Polym.* **2004**, *58*, 401.
16. Dong, Y.; Ruan, Y., Wang, H.; Zhao, Y.; Bi, D. *J. Appl. Polym. Sci.* **2004**, *93*, 1553.
17. Sakurai, K.; Maegawa, T.; Takahashi, T. *Polymer* **2000**, *41*, 7051.

18. Williamson, R. V. *J. Ind. Eng. Chem.* **1929**, *21*, 1108.
19. Focher, B.; Beltrame, P. L.; Naggi, A.; Torri, G. *Carbohydr. Polym.* **1990**, *12*, 405.
20. Crini, G.; Guibal, E.; Morcellet, M.; Torri, G.; Badot, P. M. In Chitine et Chiosane du Biopolymère à l'Application; Crini, G.; Badot, P. M.; Guibal, E., Eds.; Presses Universitaires: Franche-Comté, **2009**; Chapter 1, p 19.
21. Argüelles-Monal, W.; Goycoolea, F. M.; Peniche, C.; Higuera-Ciapara, I. *Polym Gels Netw.* **1998**, *6*, 429.
22. Cho, J.; Heuzey, M.-C.; Bégin, A.; Carreau P. J. *J. Food Eng.* **2006**, *74*, 500.
23. Garcia, A. M.; Pinotti, A.; Martino, M. N.; Zaritzky N. E. *Carbohydr. Polym.* **2004**, *56*, 339.
24. Silva-Weiss, A.; Bifani, V.; Ihl, M..; Sobral, P. J. A.; Gómez-Guillén, M. C. *Food Hydrocoll.* **2013**, *31*, 458.
25. Peshkova, S.; Li, K. *J. Biotechnol.* **2003**, *102*, 199.
26. Hernández, R.; Zamora-Mora, V.; Sibaja-Ballestero, M.; Vega-Braudit, J.; López, D.; Mijangos, C. *J. Colloid Interface Sci.* **2009**, *339*, 53.
27. Muzzarelli, R. A. A.; Greco, F.; Busilacchi, A.; Sollazzo, V.; Gigante, A. *Carbohydr. Polym.* **2012**, *89*, 723.
28. Pereda, M.; Ponce, A. G.; Marcovich, N. E.; Ruseckait, R. A.; Martucci, J. F. *Food Hydrocolloid.* **2011**, *25*, 1372.
29. Lopez, F. A.; Mercê, A. L. R.; Alguacil, F. J.; Lopez-Delgado, A. *J. Therm. Anal. Calorimetry* **2008**, *91*, 633.
30. Rubilar, J. F.; Cruz, R. M. S.; Silva, H. D.; Vicente, A. A.; Khmelinskii, I.; Vieira, M. C. *J. Food Eng.* **2013**, *115*, 466.
31. Cheung, M. K.; Wan, K. P. Y.; Yu, P. H. *J. Appl. Polym. Sci.* **2002**, *86*, 1253.
32. Ratto, J.; Hatakeyama, T.; Blumstein, R. B. *Polymer.* **1995**, *15*, 2915.
33. Mucha, M.; Pawlak, A. *Thermochim. Acta.* **2005**, *427*, 69.
34. Suyatma, N. E.; Tighzert, L.; Copinet, A.; Coma, V. *J. Agric. Food Chem.* **2005**, *53*, 3950.
35. Aziz, N. A.; Majid, S. R.; Yahya, R.; Arof, A. K. *Polym. Adv. Technol.* **2011**, *22*, 1345.
36. Martinez-Camacho, A. P.; Cortez-Rocha, M. O.; Ezquerra-Brauer, J. M.; Graciano-Verdugo, A. Z.; Rodriguez-Felix, Catillo-Ortega, M. M., Yepiz-Gomez, M. S.; Plascencia-Jatomea, M. *Carbohydr. Polym.* **2010**, *82*, 305.
37. Uragami, T.; Matsuda, T.; Okuno, H.; Miyata, T. *J. Membr. Sci.* **1994**, *88*, 243.
38. Chen, L.; Tang, C.; Ning, N.-Y.; Wang, C.-Y.; Fu, Q.; Zhang, Q. *Chin. J. Polym. Sci.* **2009**, *27*, 739.
39. Ahn, J.-S.; Choi, H.-K.; Cho, C.-S. *Biomaterials* **2001**, *22*, 923.
40. Maniukiewicz, W. In Chitin, chitosan, oligosaccharides and their derivatives: Biological activities and applications, Se-Kwon, K., Ed.; CRC Press: New York, **2010**; Chapter 8, p 83.
41. Souza, B. W. S.; Cerqueira, M. A.; Martins, J. T.; Casariego, A.; Teixeira, J. A.; Vicente, A. A. *Food Hydrocolloid* **2010**, *24*, 330.
42. Young, D. K.; No, H. K.; Prinyawiwatkul, W. *Carbohydr. Polym.* **2009**, *78*, 41.